Electronic Supplementary Material (ESI) for Journal of Materials Chemistry A.
This journal is © The Royal Society of Chemistry 2023

Supporting Information

Enabling interfacial stability of $LiCoO_2$ batteries at ultrahigh cutoff voltage ≥ 4.65 V with synergetic electrolyte strategy

Ang Fu,[a,c,1] *Chuanjing Xu,*[a,1] *Jiande Lin,*[a] *Yu Su,*[a] *Haitang Zhang,*[a,c] *De-Yin Wu,*[a] *Xiaozheng Zhang,*[a,c] *Meng Xia,*[a,c] *Zhongru Zhang,*[a] *Jianming Zheng,* *[a,c] *Yong Yang* *[a,b,c]

[a] State Key Laboratory of Physical Chemistry of Solid Surfaces, College of Chemistry and Chemical Engineering, Xiamen University, Xiamen, Fujian 361005, China.

[b] School of Energy, Xiamen University, Xiamen, Fujian 361005, China

[c] Innovation Laboratory for Sciences and Technologies of Energy Materials of Fujian Province (IKKEM), Xiamen, Fujian 361005, China

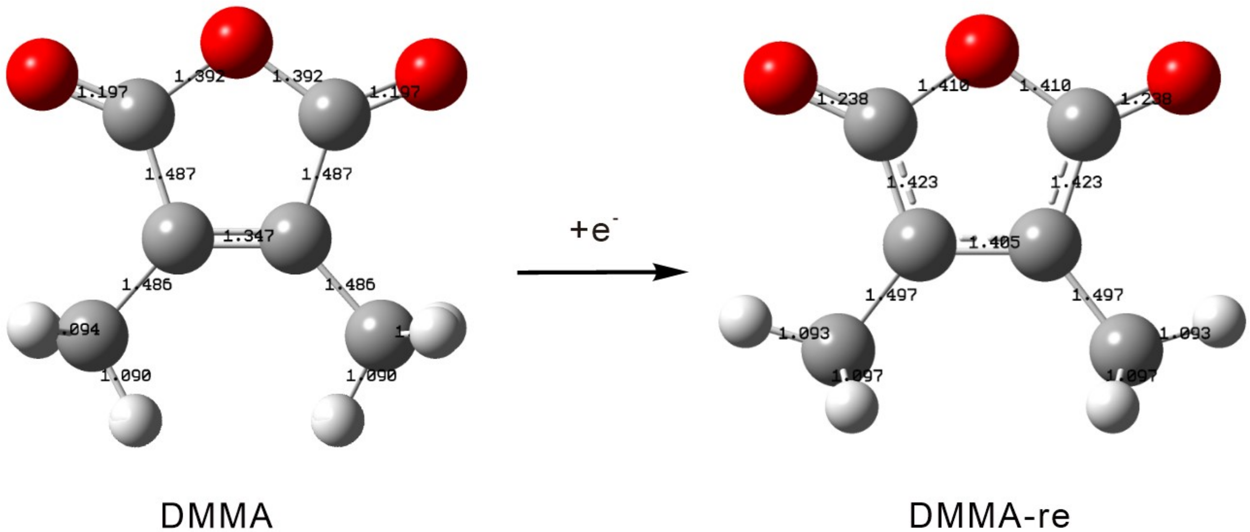

Figure S1. The configuration of DMMA and DMMA-re, and the change of bond length after DMMA accepts an electron. The calculation results show that the C=C double bond in DMMA is likely to be broken when DMMA accepts an electron.

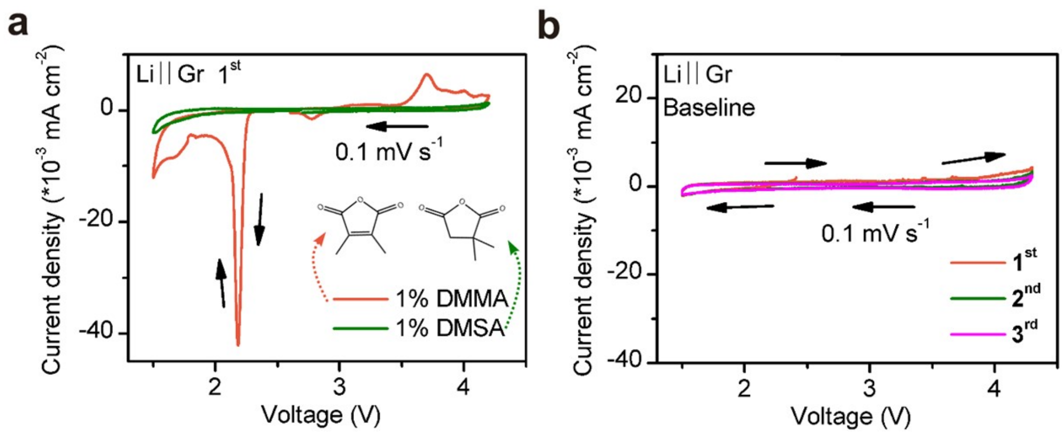

Figure S2. (a) Cyclic voltammograms of Li||Gr cells between 1.5-4.2 V in the DMMA and DMSA-containing electrolytes for the first cycle at a scanning sweep of 0.1 mV s^{-1} starting from negative scan. (b) Cyclic voltammograms of Li||Gr cell in the baseline electrolyte for 3 cycles at a scanning sweep of 0.1 mV s^{-1} starting from negative scan.

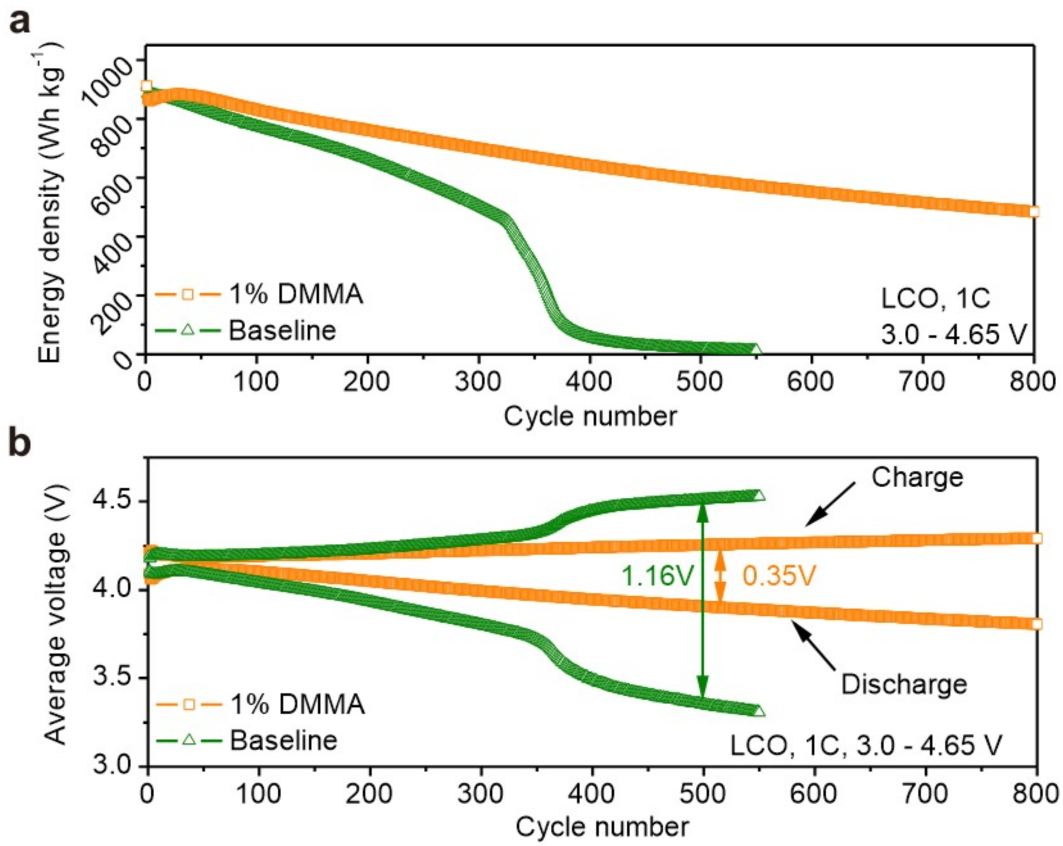

Figure S3. (a) Energy density of LCO cathodes in baseline and 1% DMMA-containing electrolytes at 1C at 30 ^{o}C in the voltage range of 3-4.65 V. (b) The corresponding mid-point charge and discharge voltages of LCO in baseline and 1% DMMA-containing electrolytes.

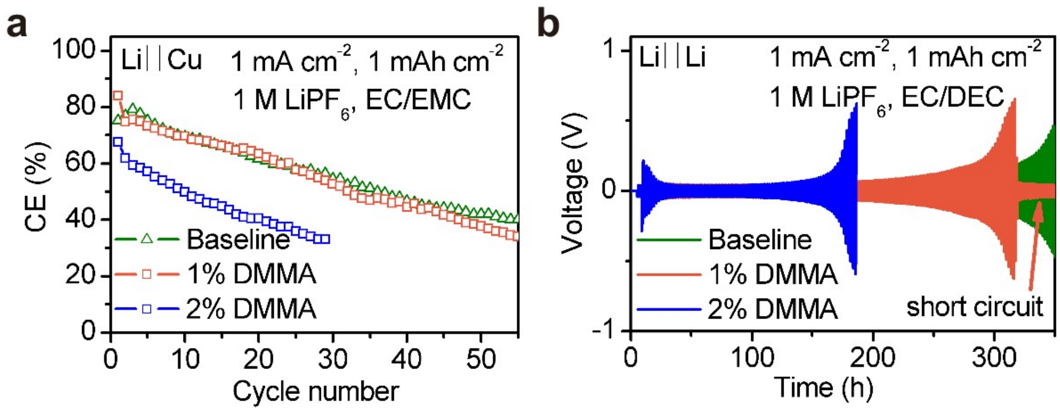

Figure S4. (a) Li cycling CEs tested in Li||Cu cells with baseline and DMMA-containing electrolytes at the current density of 1 mA cm^{-2} with the deposition capacity of 1 mAh cm^{-2}. (b) Cycling performance of symmetric Li||Li cells using baseline and DMMA-containing electrolytes at the current density of 1mA cm^{-2} with the deposition capacity of 1 mAh cm^{-2}.

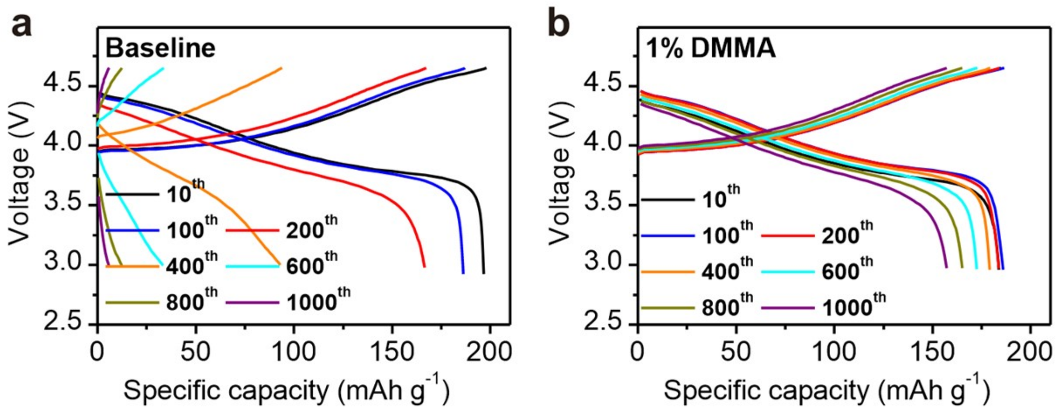

Figure S5. Charge/discharge profiles of LCO cycled in (a) baseline and (b) 1% DMMA-containing electrolytes at 2C for charge and 5C for discharge in the voltage range of 3.0-4.65 V.

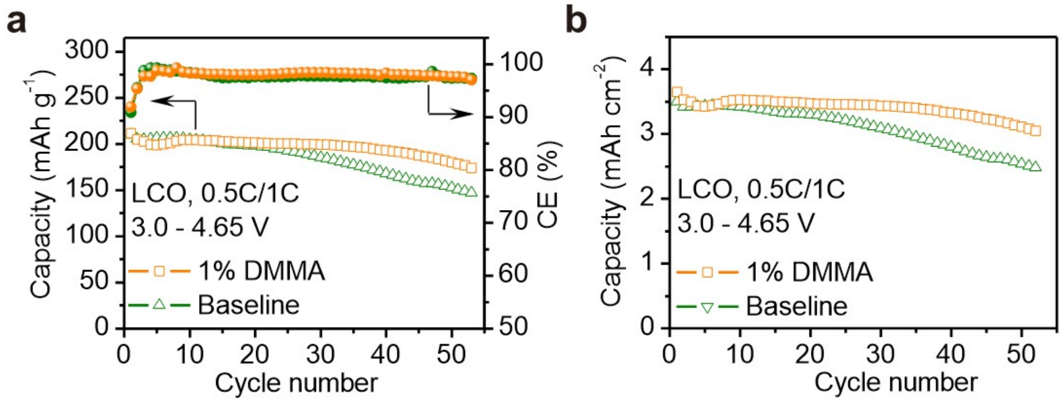

Figure S6. (a, b) Capacity as a function of cycle number of high-loading (~ 17.3 mg cm^{-2}) LCO cathode with baseline and optimized electrolytes at 3.0-4.65 V at 0.5C charge / 1C discharge rate.

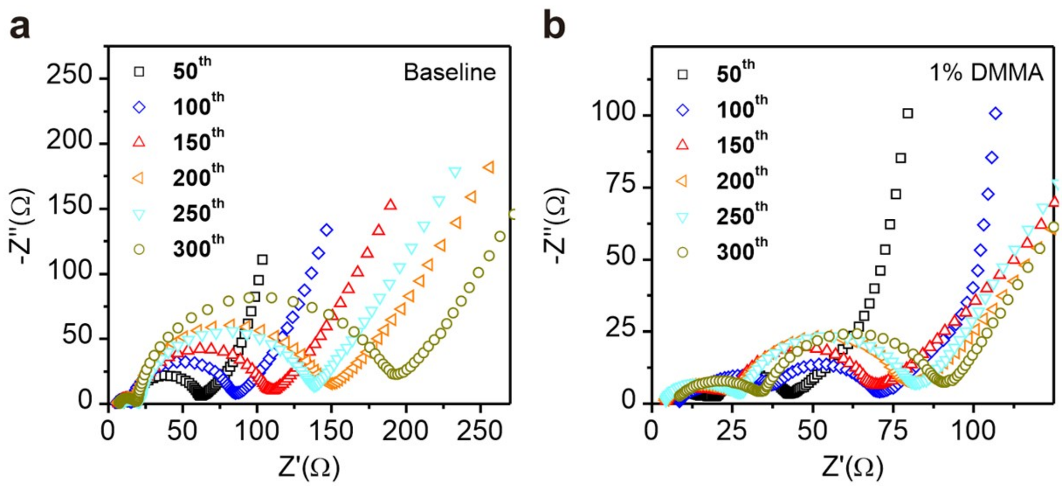

Figure S7. EIS spectra of LCO cycled in (a) baseline and (b) 1% DMMA-containing electrolytes at 50^{th}, 100^{th}, 150^{th}, 200^{th}, 250^{th}, and 300^{th} cycles at 1C and 30 ^{o}C in the voltage range of 3.0-4.65 V.

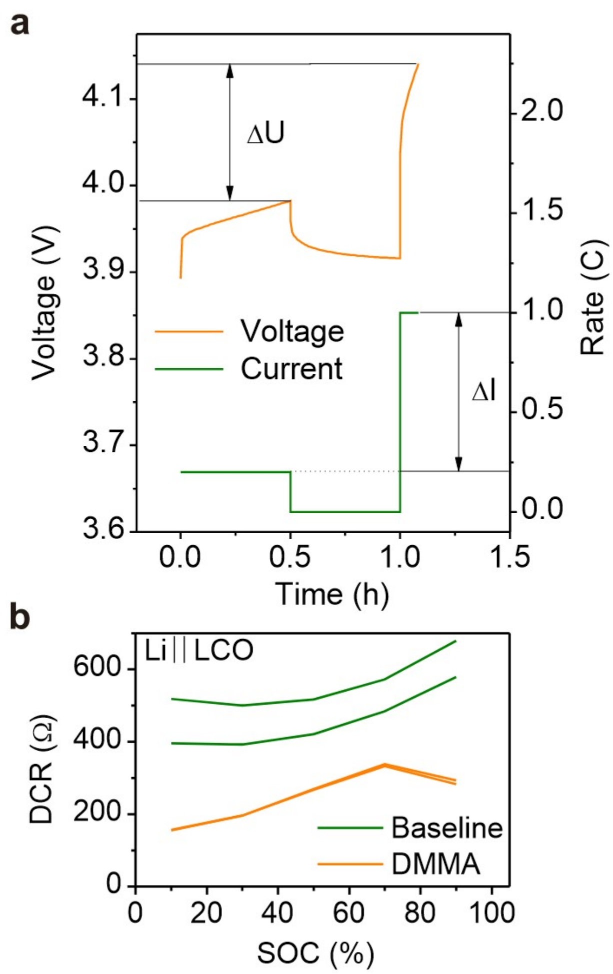

Figure S8. (a) Illustration of procedure used for DCR measurement. $R = \Delta U/\Delta I$, where ΔU is the voltage change in different charge current densities, and the ΔI is the difference between 0.2C and 1C (1C = 200 mA g^{-1}). (b) DCR values of LCO operated in baseline and 1% DMMA-containing electrolytes at different states of charge (SOCs) after 200 cycles.

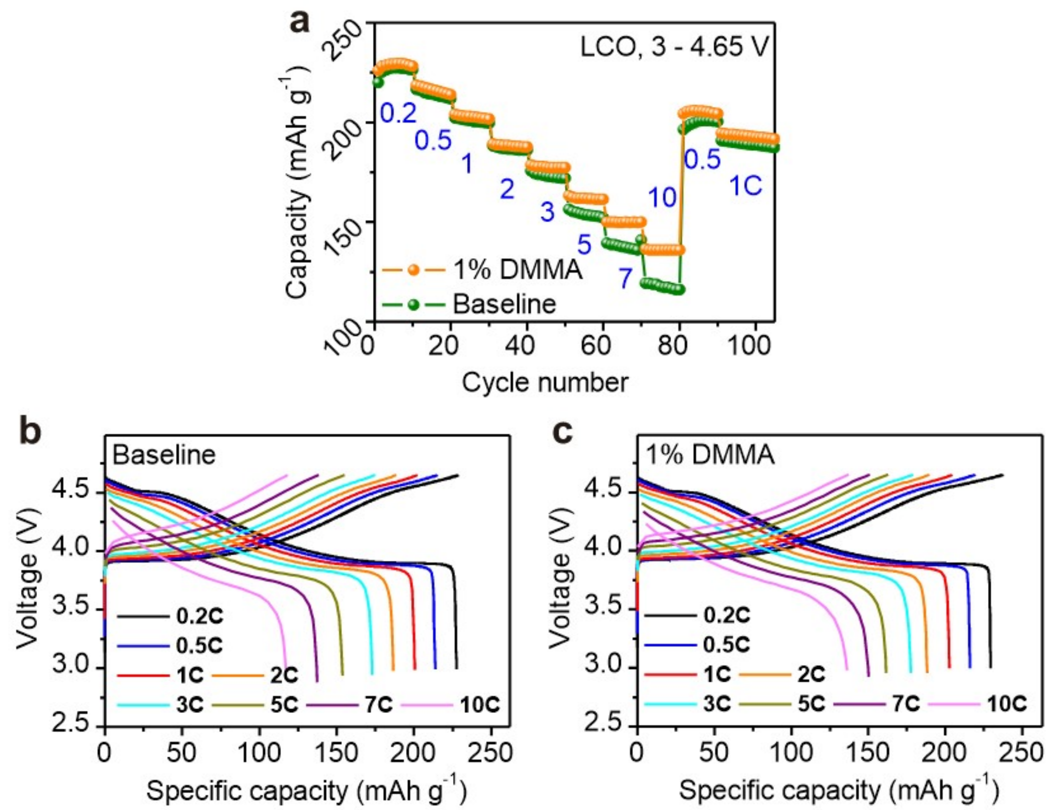

Figure S9. (a) Rate performance of LCO with baseline and 1% DMMA-containing electrolytes at 0.2, 0.5, 1, 2, 3, 5, 7, and 10C in the voltage range of 3.0-4.65 V. (b, c) The corresponding charge/discharge curves in (b) baseline and (c) 1% DMMA-containing electrolytes.

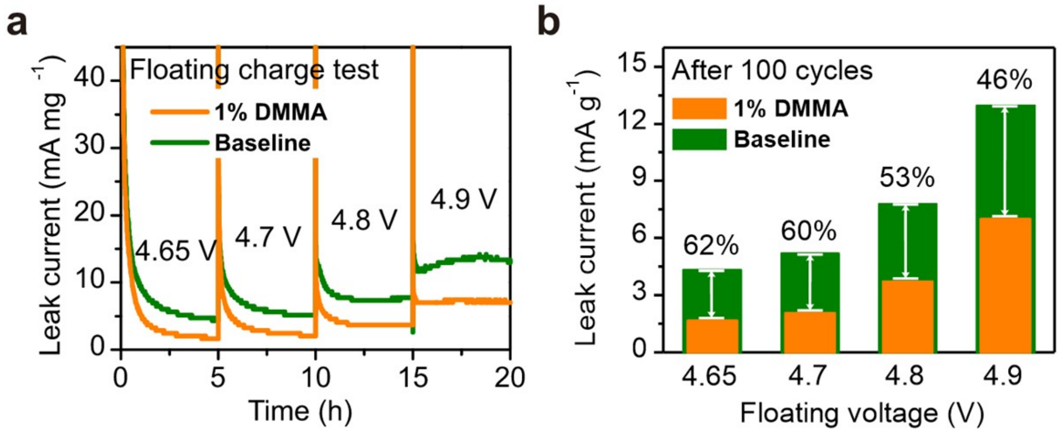

Figure S10. (a, b) Amperometry (floating charge) test of LCO batteries at 4.65, 4.7, 4.8 and 4.9 V at 45 ^{o}C after 100 cycles in the voltage range of 3.0-4.65 V.

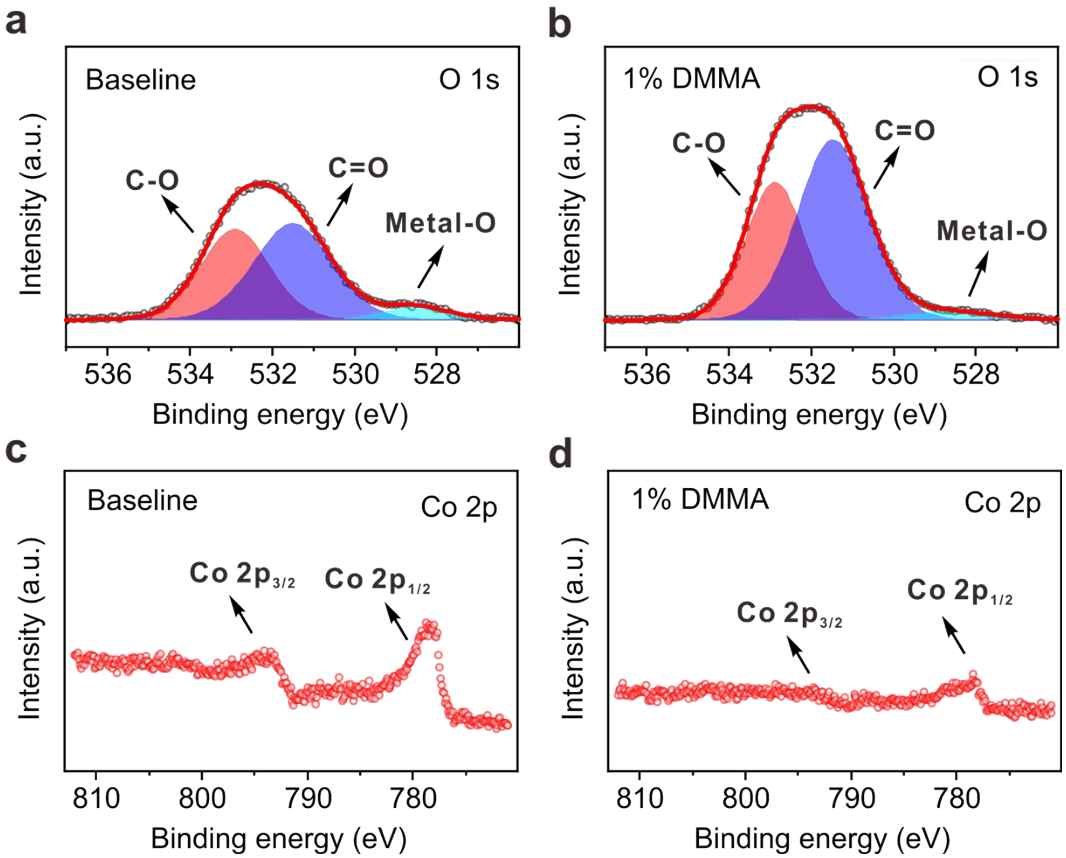

Figure S11. O 1s XPS spectra of LCO surface after cycling for 200 cycles in (a) baseline and (b) 1% DMMA-containing electrolytes. (c, d) Co 2p XPS spectra of LCO cathodes after cycling for 200 cycles in (c) baseline and (d) 1% DMMA-containing electrolytes.

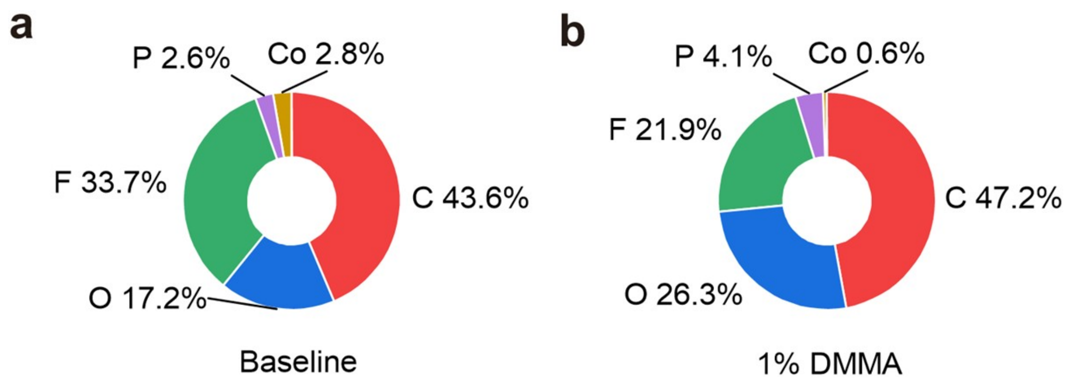

Figure S12. The comparison of element percentage of CEI film at LCO surface after cycling (at 1C and cutoff 4.65 V for 200 cycles) in (a) baseline and (b) 1% DMMA-containing electrolytes obtained from XPS results.

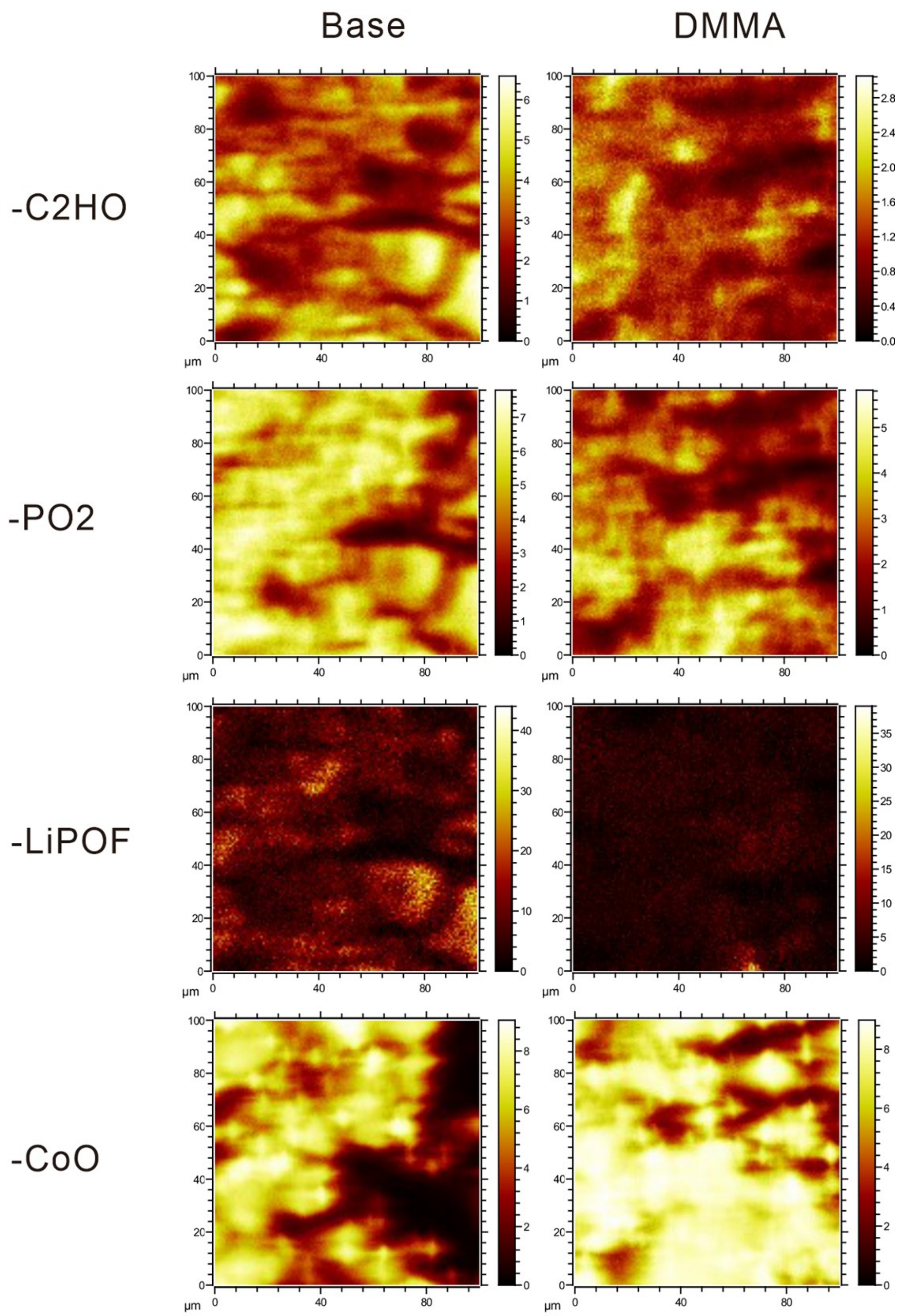

Figure S13. The comparison of element percentage of CEI film at LCO surface after cycling (at 1C and cutoff 4.65 V for 200 cycles) in (a) baseline and (b) 1% DMMA-containing electrolytes obtained from XPS results.

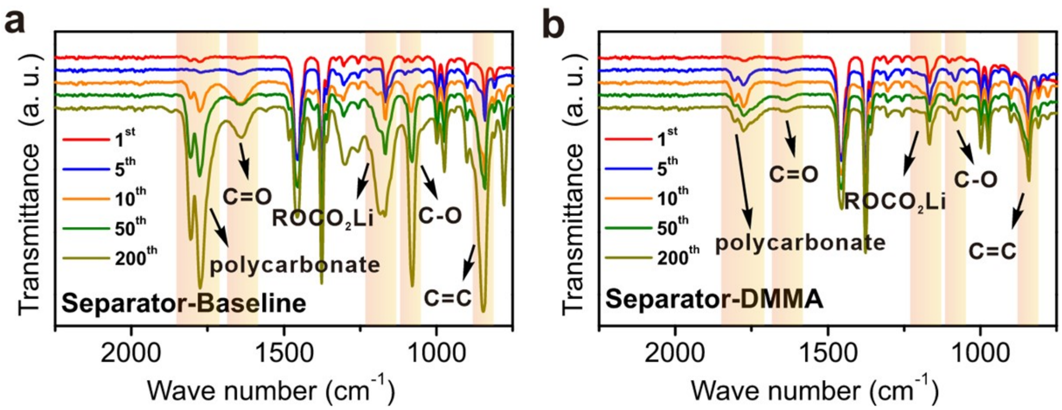

Figure S14. FTIR spectra of separators disassembled from LCO batteries cycled in (a) baseline and (b) optimized electrolytes.

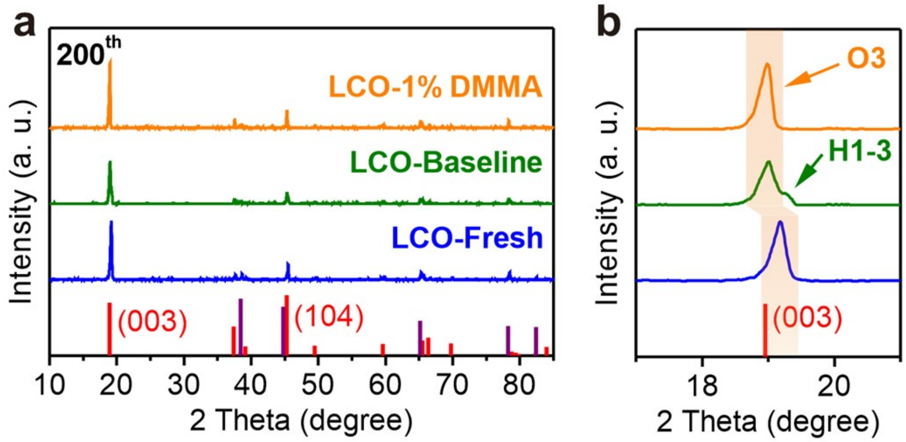

Figure S15. XRD patterns of fresh LCO and the LCO cycled in baseline and 1% DMMA-containing electrolytes at 1C and cutoff 4.65 V (discharge state at 200th cycle).

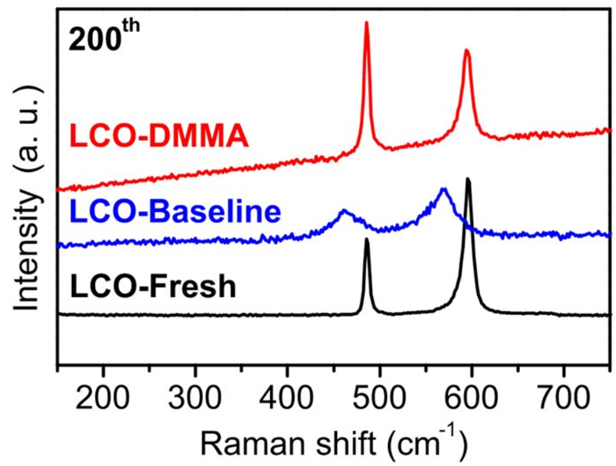

Figure S16. Raman spectra of fresh LCO and the LCO cycled in (a) baseline and (b) 1% DMMA-containing electrolytes at 1C and 30 ^{o}C in the voltage range of 3.0-4.65 V.

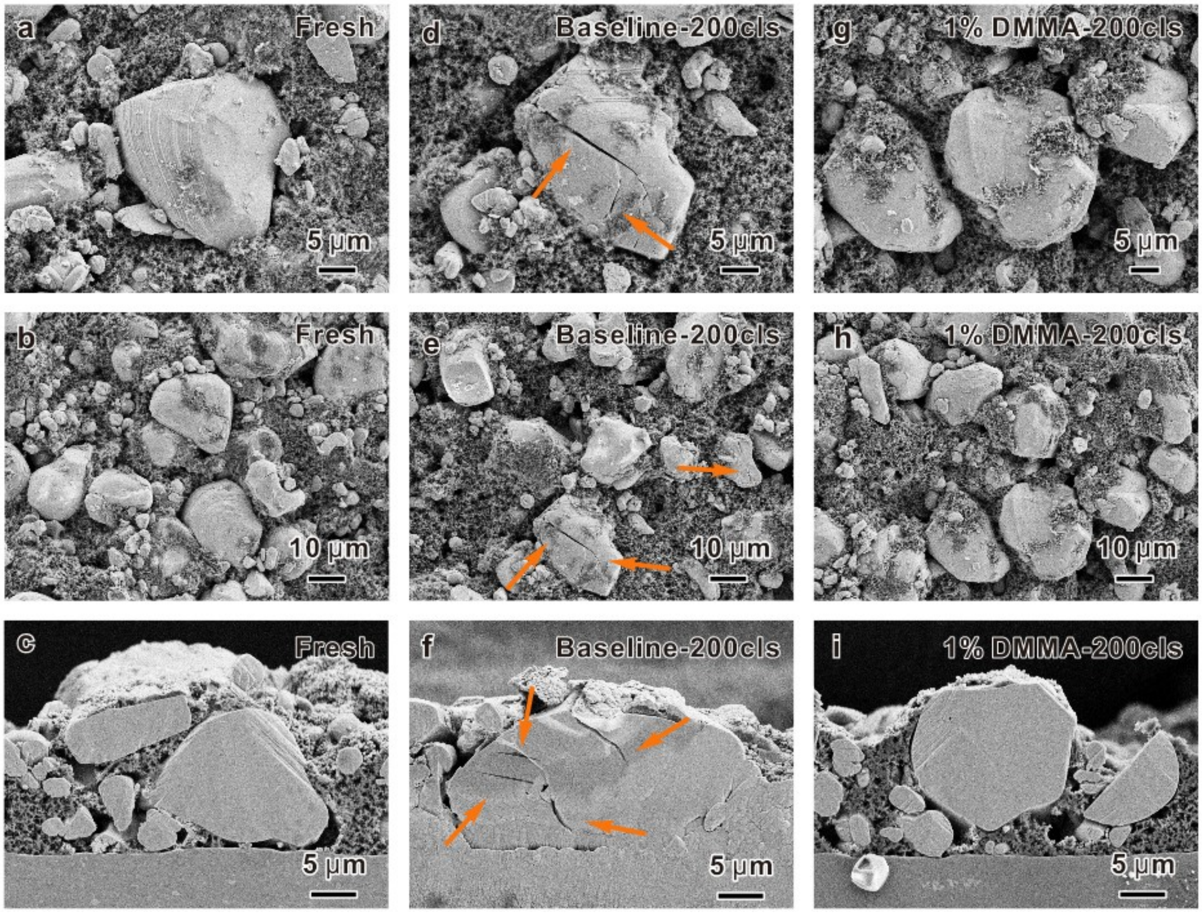

Figure S17. SEM images of the surface and cross-sectional morphologies of (a-c) fresh LCO cathode, and the LCO cathodes cycled at 1C and cutoff 4.65 V for 200 cycles in (d-f) baseline and (g-i) optimized electrolytes at different regions.

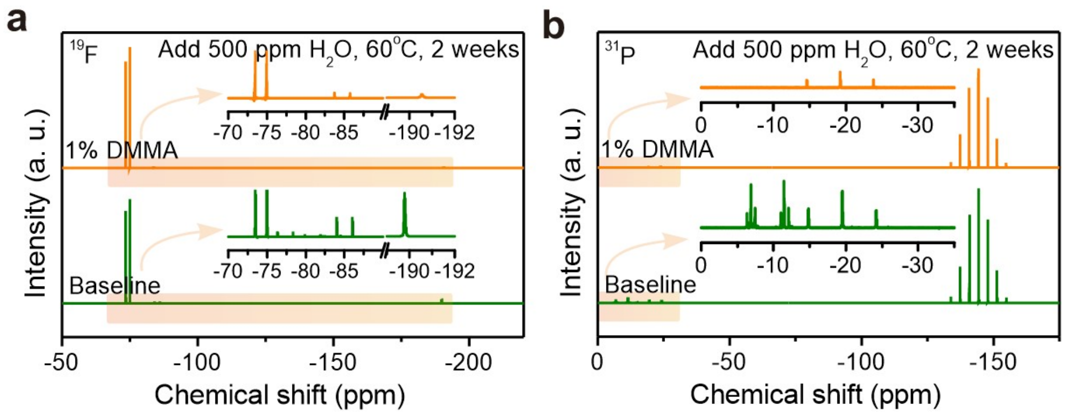

Figure S18. NMR spectra of (a) ^{19}F and (b) ^{31}P of baseline and 1% DMMA-containing electrolytes added with 500 ppm H_2O and stored at 60 ^{o}C for 2 weeks.

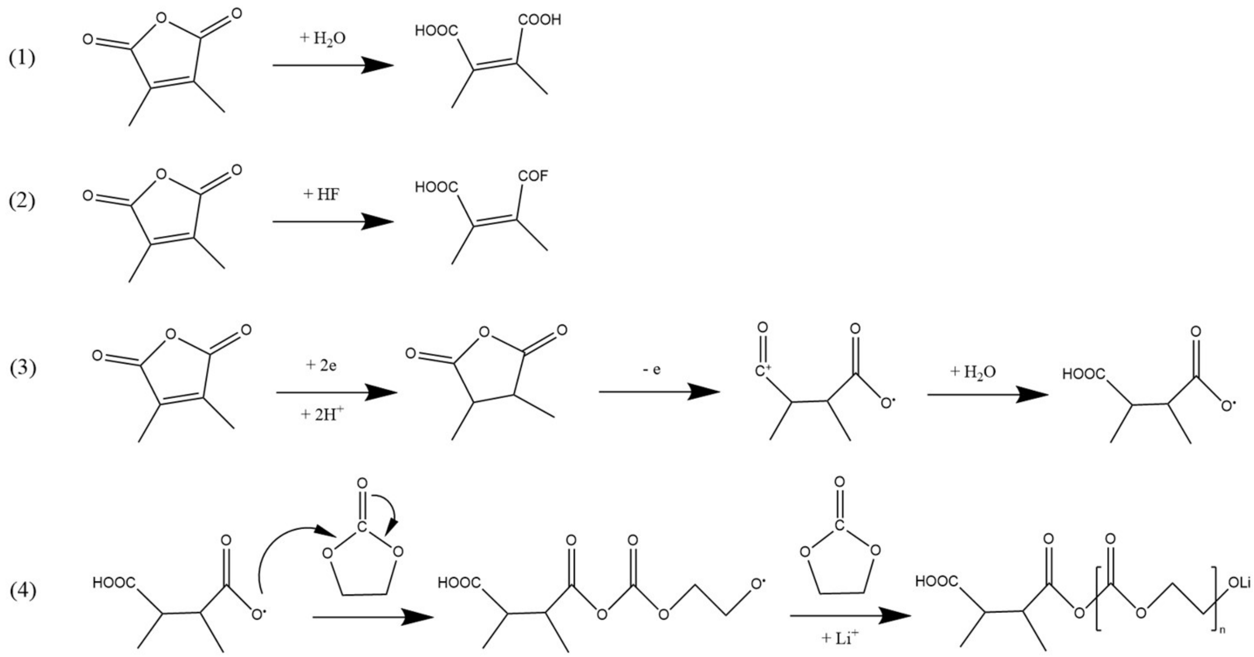

Figure S19. The possible reaction mechanisms of DMMA additive.

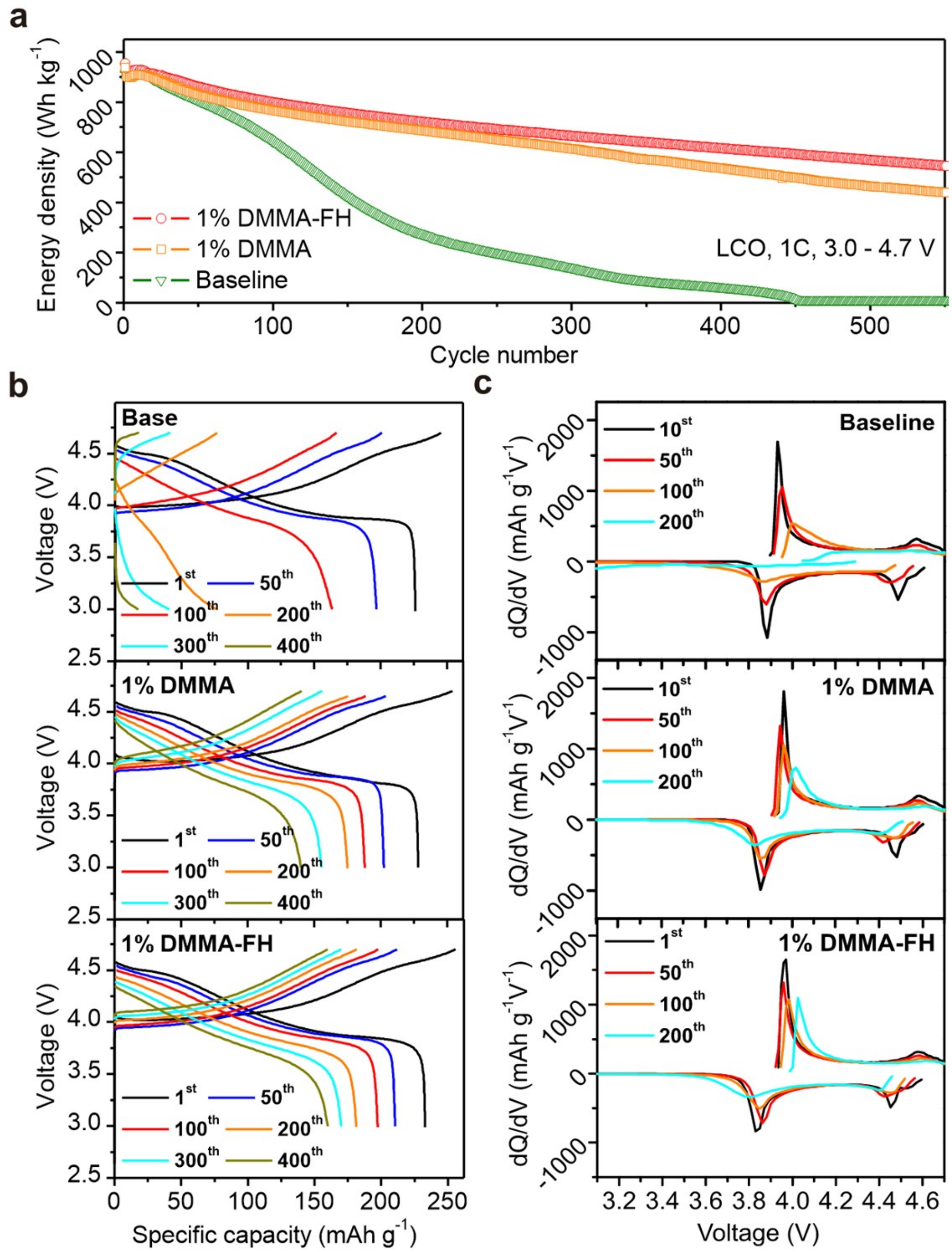

Figure S20. (a) Energy density as a function of cycle number of LCO with baseline, optimized (adding 1% DMMA) and upgraded (adding 1% DMMA, 5% FEC, and 1% HTCN) electrolytes at 3.0-4.7 V at 1C. (b) The corresponding charge/discharge curves and (c) dQ/dV profiles at selected cycles in the different electrolytes.

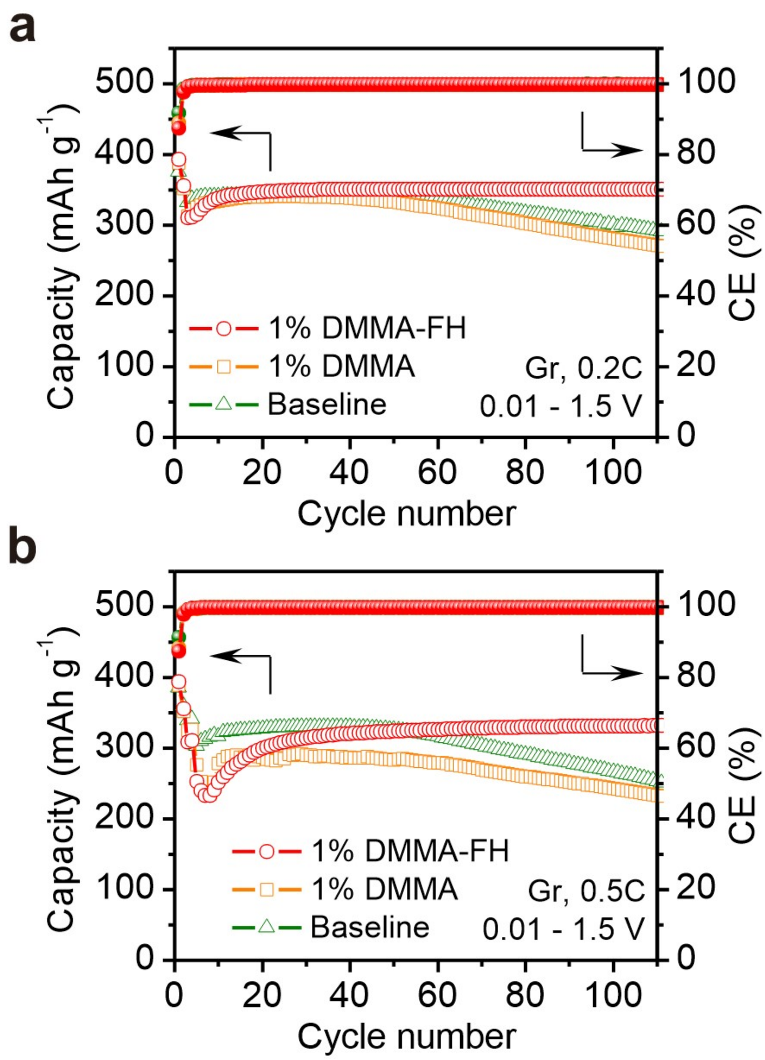

Figure S21. Cycling performance of Li||Gr half batteries with baseline, optimized (adding 1% DMMA) and upgraded (adding 1% DMMA, 5% FEC, and 1% HTCN) electrolytes at (a) 0.2C and (b) 0.5C in the voltage range of 0.01-1.5 V.

Table S1. Comparison of electrochemical performance of the electrolyte additives and recipes reported for high-voltage LCO batteries.

Electrolyte additives and recipes	Capacity retention (%)	Voltage range (V)	Areal loading (mg cm^{-2})	Current rate or density (C or mA g^{-1})	Ref.
5-Acetylthiophene-2-carbonitrile	91 (200th)	3-4.5	2.3–2.6	180	1
Di(methylsulfonyl) ethane	66.5 (100th)	3-4.5	15.4	1C	2
Tris(2-cyanoethyl) borate	78.2 (200th)	2.75-4.5	2	180	3
Dihydro-1,3,2-dioxathiolo[1,3,2]dioxathiole 2,2,5,5-tetraoxide	77.7 (250th)	3.0-4.5	1.86	0.7C	4
Aluminum isopropoxide	78.1 (200th)	3-4.6	5	200	5
Fluoroethylene carbonate (FEC) and 1,3,6-hexanetricarbonitrile (HTCN)	75 (300th)	3-4.6	6	200	6
Triisopropanolamine cyclic borate	82.2 (200th)	3-4.6	2-3	200	7
	85.2 (100th)	**3-4.65**	2-3	200	
2.4.6-Tris(4-fluorophenyl)boroxin	84.6 (200th)	3-4.6	2-3	200	8
	65.8 (200th)	**3-4.65**	2-3	200	
	74 (85th)	**3-4.7**	2-3	200	
4-Methylmorpholine-	83.5 (200th)	3-4.6	2-3	200	9

2,6-dione	**72.3 (200th)** **55.4 (200th)**	**3-4.65** **3-4.7**	2-3 2-3	200 200	
KSeCN	55.2 (750th)	3-4.6	3	200	10
Potassium (4-methylsulfonylphenyl) trifluoroborate	**70.3 (300th)**	**3-4.65**	3	200	11
Vinylene carbonate and KBF_4	91.9 (300th)	3-4.6	~5	274	12
1M LiFSI, in N,N-dimethyltrifluoromet-hanesulfonamide	89 (200th) 85 (100th)	3-4.55 3-4.6	~13 ~13	150 150	13
1 M $LiPF_6$ in FEC/FEMC/TTE +2 wt% TMSB	74.8 (300th)	3-4.6	~18	137	14
0.3 M LiDFOB + 0.2 M $LiBF_4$ in DEC/FEC/FB	85.6 (120th)	3-4.6	20.4	49	15
2,3-Dimethylmaleic anhydride (DMMA)	**70.7 (500th)** **69.4 (400th)** **69.6 (300th)**	**3-4.65** **3-4.65** **3-4.7**	**~3** **~8** **~3**	**200** **200** **200**	**This work**
1M $LiPF_6$, in EC/EMC, + 1% DMMA, 5% FEC, and 1% HTCN	**75.9 (300th)**	**3-4.7**	**~3**	**200**	**This work**

Table S2. Comparison of electrochemical performance of this research with the modified LCO at the cutoff voltage over 4.6 V.

Modified LCO	Capacity retention (%)	Voltage range (V)	Areal loading (mg cm^{-2})	Current rate or density (C or mA g^{-1})	Ref.
Al, Ti-bulk doped and Mg-surface doped LCO	78 (300^{th})	3-4.6	~1.5	70	16
Ti, Mg, Al co-doped LCO	86 (100^{th})	3-4.6	--	137	17
Mg-pillared LCO	84 (100^{th})	3-4.6	~3	270	18
MgF_2-doped LCO	92 (100^{th})	3-4.6	~3	270	19
Al, F co-doped LCO	86.9 (200^{th})	3-4.6	~3	100	20
Al, F, Mg gradient co-doped LCO	80.9 (500^{th})	3-4.6	~3	137	21
Ni, P co-doped LCO	92.6 (100^{th})	3-4.6	4.2-4.6	137	22
$Li_2SO_4/Li_xCo_2O_4$ coated and trace S-doped LCO	88 (100^{th})	2.8-4.6	2	280	23
Li, Al, F-modified LCO	91 (200^{th})	3-4.6	~12.6	27.4	24
$AlPO_4$ and Li_3PO_4 co-coated LCO	88.6 (200^{th}) 79.7 (400^{th})	3-4.6	3-4	137	25
$Li_{1.5}Al_{0.5}Ti_{1.5}(PO_4)_3$-coated LCO	88.3 (100^{th})	3-4.6	3	137	26
Surface Se-substituted LCO	86.7 (120^{th})	3-4.62	16-17	70	27
Al-doped ZnO and $Li_{1.5}Al_{0.5}Ge_{1.5}P_3O_{12}$ co-coated LCO	77.1 (300^{th})	3-4.6	2	185	28
AlZnO-coated LCO	65.7 (500^{th})	3-4.6	--	185	29

TiO_2 and LiF co-coated LCO	85.4 (100^{th})	3-4.6	--	70	30
Al_2O_3-coated LCO (by ALD method)	88 (200^{th})	3-4.6	2	95	31
LiF, KF, and $LiCo_{1-x}Al_xO_2$ modified LCO	78.7 (100^{th}) **60.4 (200^{th})**	3-4.6 **3-4.7**	-- --	0.5C 0.5C	32
F-surface doped and LiF/$Li_2CoTi_3O_8$ coated LCO	82.5 (100^{th}) 81.2 (200^{th})	3-4.6 3-4.6	8-9 8-9	137 27.4	33
Mg-doped and Co_xB_y-coated LCO	94.6 (100^{th})	3-4.6	2.5	270	34
Mg-doped and Se-coated LCO	72.9 (1000^{th}) **68.6 (400^{th})** **80.7 (100^{th})**	3-4.6 **3-4.65** **3-4.7**	~3	200 200 200	35
Li, Al, F-modified LCO combining with optimized electrolyte (1M $LiPF_6$, in FEC/DFEC/DMC)	77.8 (500^{th})	3-4.6	--	110	36
$RbAlF_4$-modified LCO with optimized electrolyte (1M $LiPF_6$, in FEC/DFEC/DMC)	91.5 (100^{th}) 80.2 (500^{th}) **82 (100^{th})** **76 (100^{th})**	3-4.6 3-4.6 **3-4.65** **3-4.7**	~6	110	37
Coherent $LiCoPO_4$-coated LCO combining with optimized electrolyte (1M $LiPF_6$, in EC/EMC, + 5% FEC, +1% SUN)	87 (300^{th}) **83 (100^{th})**	3-4.6 **3-4.7**	~3 ~3	200 200	38

REFERENCES

1. D. Ruan, M. Chen, X. Wen, S. Li, X. Zhou, Y. Che, J. Chen, W. Xiang, S. Li, H. Wang, X. Liu and W. Li, *Nano Energy*, 2021, **90**, 106535.
2. X. Zheng, T. Huang, G. Fang, Y. Pan, Q. Li and M. Wu, *ACS Appl. Mater. Interfaces*, 2019, **11**, 36244-36251.
3. Z. Zhang, F. Liu, Z. Huang, J. Gu, Y. Song, J. Zheng, M. Yi, Q. Mao, M. Bai, X. Fan, B. Hong, Z. Zhang and Y. Lai, *ACS Appl. Energy Mater.*, 2021, **4**, 12954-12964.
4. X. Q. Liao, F. Li, C. M. Zhang, Z. L. Yin, G. C. Liu and J. G. Yu, *Nanomaterials*, 2021, **11**, 609.
5. J. Yang, X. Liu, Y. Wang, X. Zhou, L. Weng, Y. Liu, Y. Ren, C. Zhao, M. Dahbi, J. Alami, D. A. Ei-Hady, G. L. Xu, K. Amine and M. Shao, *Adv. Energy Mater.*, 2021, **11**, 2101956.
6. X. Yang, M. Lin, G. Zheng, J. Wu, X. Wang, F. Ren, W. Zhang, Y. Liao, W. Zhao, Z. Zhang, N. Xu, W. Yang and Y. Yang, *Adv. Funct. Mater.*, 2020, **30**, 2004664.
7. Y. Zou, Y. Cheng, J. Lin, Y. Xiao, F. Ren, K. Zhou, M.-S. Wang, D.-Y. Wu, Y. Yang and J. Zheng, *J. Power Sources*, 2022, **532**, 231372.
8. Y. Zou, A. Fu, J. Zhang, T. Jiao, Y. Yang and J. Zheng, *ACS Sustain. Chem. Eng.*, 2021, **9**, 15042-15052.
9. Y. Zou, J. Zhang, J. Lin, D.-Y. Wu, Y. Yang and J. Zheng, *J. Power Sources*, 2022, **524**, 231049.
10. A. Fu, J. Lin, Z. Zhang, C. Xu, Y. Zou, C. Liu, P. Yan, D.-Y. Wu, Y. Yang and J. Zheng, *ACS Energy Lett.*, 2022, **7**, 1364-1373.

11. Y. Yan, S. Weng, A. Fu, H. Zhang, J. Chen, Q. Zheng, B. Zhang, S. Zhou, H. Yan, C.-W. Wang, Y. Tang, H. Luo, B.-W. Mao, J. Zheng, X. Wang, Y. Qiao, Y. Yang and S.-G. Sun, *ACS Energy Lett.*, 2022, **7**, 2677-2684.

12. K. Zhang, J. Chen, W. Feng, C. Wang, Y.-N. Zhou and Y. Xia, *J. Power Sources*, 2023, **553**, 232311.

13. W. Xue, R. Gao, Z. Shi, X. Xiao, W. Zhang, Y. Zhang, Y. G. Zhu, I. Waluyo, Y. Li, M. R. Hill, Z. Zhu, S. Li, O. Kuznetsov, Y. Zhang, W.-K. Lee, A. Hunt, A. Harutyunyan, Y. Shao-Horn, J. A. Johnson and J. Li, *Energy Environ. Sci.*, 2021, **14**, 6030-6040.

14. J. Zhang, P. F. Wang, P. Bai, H. Wan, S. Liu, S. Hou, X. Pu, J. Xia, W. Zhang, Z. Wang, B. Nan, X. Zhang, J. Xu and C. Wang, *Adv. Mater.*, 2021, **34**, 2108353.

15. Z. Jiang, Z. Zeng, H. Zhang, L. Yang, W. Hu, X. Liang, J. Feng, C. Yu, S. Cheng and J. Xie, *iScience*, 2022, **25**, 103490.

16. L. Wang, J. Ma, C. Wang, X. Yu, R. Liu, F. Jiang, X. Sun, A. Du, X. Zhou and G. Cui, *Adv. Sci.*, 2019, **6**, 1900355.

17. J.-N. Zhang, Q. Li, C. Ouyang, X. Yu, M. Ge, X. Huang, E. Hu, C. Ma, S. Li, R. Xiao, W. Yang, Y. Chu, Y. Liu, H. Yu, X.-Q. Yang, X. Huang, L. Chen and H. Li, *Nat. Energy*, 2019, **4**, 594-603.

18. Y. Huang, Y. Zhu, H. Fu, M. Ou, C. Hu, S. Yu, Z. Hu, C. T. Chen, G. Jiang, H. Gu, H. Lin, W. Luo and Y. Huang, *Angew. Chem. Int. Ed.*, 2020, **133**, 4732-4738.

19. W. Kong, J. Zhang, D. Wong, W. Yang, J. Yang, C. Schulze and X. Liu, *Angew Chem. Int. Ed.*, 2021, **133**, 27308–27318.

20. W. Huang, Q. Zhao, M. Zhang, S. Xu, H. Xue, C. Zhu, J. Fang, W. Zhao, G. Ren, R. Qin, Q. Zhao, H. Chen and F. Pan, *Adv. Energy Mater.*, 2022, **12**, 2200813.

21. Y. He, X. Ding, T. Cheng, H. Cheng, M. Liu, Z. Feng, Y. Huang, M. Ge, Y. Lyu and B. Guo, *J. Energy Chem.*, 2023, **77**, 553-560.

22. N. Qin, Q. Gan, Z. Zhuang, Y. Wang, Y. Li, Z. Li, H. Iftikhar, C. Zeng, G. Liu, Y. Bai, K. Zhang and Z. Lu, *Adv. Energy Mater.*, 2022, **12**, 2201549.

23. X. Tan, T. Zhao, L. Song, D. Mao, Y. Zhang, Z. Fan, H. Wang and W. Chu, *Adv. Energy Mater.*, 2022, **12**, 2200008.

24. J. Qian, L. Liu, J. Yang, S. Li, X. Wang, H. L. Zhuang and Y. Lu, *Nat. Commun.*, 2018, **9**, 4918.

25. X. Wang, Q. Wu, S. Li, Z. Tong, D. Wang, H. L. Zhuang, X. Wang and Y. Lu, *Energy Stor. Mater.*, 2021, **37**, 67-76.

26. Y. Wang, Q. Zhang, Z. C. Xue, L. Yang, J. Wang, F. Meng, Q. Li, H. Pan, J. N. Zhang, Z. Jiang, W. Yang, X. Yu, L. Gu and H. Li, *Adv. Energy Mater.*, 2020, **10**, 2001413.

27. Z. Zhu, H. Wang, Y. Li, R. Gao, X. Xiao, Q. Yu, C. Wang, I. Waluyo, J. Ding, A. Hunt and J. Li, *Adv. Mater.*, 2020, **32**, 2005182.

28. T. Cheng, Q. Cheng, Y. He, M. Ge, Z. Feng, P. Li, Y. Huang, J. Zheng, Y. Lyu and B. Guo, *ACS Appl. Mater. Interfaces*, 2021, **13**, 42917-42926.

29. T. Cheng, Z. Ma, R. Qian, Y. Wang, Q. Cheng, Y. Lyu, A. Nie and B. Guo, *Adv. Funct. Mater.*, 2021, **31**, 2001974.

30. Z. Wang, X. Dai, H. Chen, F. Wu, Y. Mai, S. Li, Y. Gu, J. Li and A. Zhou, *ACS Sustain. Chem. Eng.*, 2022, **10**, 8151-8161.

31. R. Wu, T. Cao, H. Liu, X. Cheng, X. Liu and Y. Zhang, *ACS Appl. Mater. Interfaces*, 2022, **14**, 25524-25533.

32. Y. Liao, Z. Wang, X. Dai, H. Chen, F. Wu, J. Li, Y. Mai and S. Li, *J. Phys. Chem. C*, 2022, **126**, 16627-16635.

33. S. Mao, Z. Shen, W. Zhang, Q. Wu, Z. Wang and Y. Lu, *Adv. Sci.*, 2022, **9**, 2104841.

34. J. Chen, H. Chen, S. Zhang, A. Dai, T. Li, Y. Mei, L. Ni, X. Gao, W. Deng, L. Yu, G. Zou, H. Hou, M. Dahbi, W. Xu, J. Wen, J. Alami, T. Liu, K. Amine and X. Ji, *Adv. Mater.*, 2022, **34**, 2204845.

35. A. Fu, Z. Zhang, J. Lin, Y. Zou, C. Qin, C. Xu, P. Yan, K. Zhou, J. Hao, X. Yang, Y. Cheng, D.-Y. Wu, Y. Yang, M.-S. Wang and J. Zheng, *Energy Stor. Mater.*, 2022, **46**, 406-416.

36. T. Fan, W. Kai, V. K. Harika, C. Liu, A. Nimkar, N. Leifer, S. Maiti, J. Grinblat, M. N. Tsubery, X. Liu, M. Wang, L. Xu, Y. Lu, Y. Min, N. Shpigel and D. Aurbach, *Adv. Funct. Mater.*, 2022, **32**, 2204972.

37. T. Fan, Y. Wang, V. K. Harika, A. Nimkar, K. Wang, X. Liu, M. Wang, L. Xu, Y. Elias, H. Scalar, M. S. Chae, Y. Min, Y. Lu, N. Shpigel and D. Aurbach, *Adv. Sci.*, 2022, **9**, 2202627.

38. X. Yang, C. Wang, P. Yan, T. Jiao, J. Hao, Y. Jiang, F. Ren, W. Zhang, J. Zheng, Y. Cheng, X. Wang, W. Yang, J. Zhu, S. Pan, M. Lin, L. Zeng, Z. Gong, J. Li and Y. Yang, *Adv. Energy Mater.*, 2022, **12**, 2200197.